Nuclear Physics A471 (1987) 427c-448c
North-Holland, Amsterdam

COMPUTER SIMULATIONS OF FRAGMENTATION

Glenn E. BEAUVAIS, David H. BOAL and James GLOSLI

Dept. of Physics, Simon Fraser University, Burnaby, B.C., Canada V5A 1S6

A semiclassical model for describing nuclear reactions at intermediate energy is presented. The model is applied to the study of fragmentation in proton and heavy ion induced reactions. Computer simulations based on the model allow one to follow the evolution of the reactions in both coordinate and phase space. The reaction trajectories are found to be influenced by the existence of a mechanical instability region at a density of less than half normal nuclear matter density.

1. INTRODUCTION

The problem of developing a description of nuclear reactions is a difficult one for several reasons. The systems are small and the reaction regions are inhomogeneous. Except under certain limits, quantum mechanical effects and the fermionic nature of the nuclear constituents can be expected to complicate a simple classical description. Such systems, while difficult to handle analytically, are possible to handle via computer simulations.

Numerical simulation techniques have been applied to nuclear physics problems for about four decades. Several approaches have been developed, each with its own area of applicability (for a general review see reference 1). The methods range from the cascade model, which solves the classical A-body problem[2], through Boltzmann-like equations for the evolution of 1-body distributions[3,4], to the solution of the hydrodynamic equations for integrated quantities such as the energy and baryon number densities[5]. The study of nuclear fragmentation requires elements from many of these approaches: one needs the A-body nature of the cascade approach as well as the nuclear binding and Pauli blocking effects which have been incorporated in the Boltzmann-like approaches. In this paper, we will use a semiclassical model[6,7] (see also references 8-10) in which the nucleon equations of motion are integrated classically while effects arising from Fermi-Dirac statistics are incorporated through a collision term which evaluates the occupancy of phase space available to colliding nucleons.

There are, of course, many different problems in fragmentation and reaction mechanism studies which one can address by means of computer simulations. Here, we will concentrate on the physics of the nuclear matter liquid/gas phase transition and its effect on the production of fragments in nuclear reactions.

In Section 2, we outline the basis of the simulation which we use in attacking these questions: we show the kinds of experimental observables that can be calculated in the simulations and try to develop an intuitive picture of intermediate energy reactions by showing the predicted time evolution of three selected central collisions: p + Ag at 300 MeV, Ca + Ca at 25 and 50 MeV/nucleon. In Section 3, the physics of the liquid/gas phase transition is outlined and its possible importance for reaction studies is discussed. Section 4 contains results from the study of reaction trajectories in phase and coordinate space. It is demonstrated that phase transition-like effects are observable in the trajectories, although the relationship between these effects and those expected in infinite neutral nuclear matter is not yet clear. A summary is contained in Section 5.

2. A MODEL FOR FRAGMENTATION

The model which we wish to use to investigate fragmentation phenomena is one based on classical mechanics. The individual nucleons are assigned positions and momenta which are updated at finite time intervals. The force to which the nucleons are subjected is calculated from a density dependent mean field, which has the form:

$$(1) \qquad U(\rho) = a\rho + b\rho^2 + c\varepsilon_i \frac{\rho_p - \rho_n}{\rho_o}$$

The parameters a, b and c are assigned the values -124, 70.5 and 25 MeV. Normal nuclear matter density is denoted by ρ_o (equal to 0.15 here) while the individual proton and neutron densities are denoted by ρ_p and ρ_n. The isospin-dependent term contains an element ε_i which is equal to +1 for protons and -1 for neutrons. Unlike one-body kinetic equations such as the Boltzmann or Vlasov equations, here we wish to keep the fluctuations and simulate the dynamics on an event-by-event basis. Clearly, point nucleons are not appropriate mathematically (or appropriate physically) for the evaluation of densities when there are so few particles in the system. Hence, for the purpose of evaluating the nucleons' density in coordinate and phase space, we spread out their probability density with a Gaussian function

$$(2) \qquad \exp\left\{-[(\alpha\Delta r)^2 + (\Delta p/\alpha)^2]\right\}$$

where Δr and Δp are the differences in position and momentum between the classically assigned values of a given nucleon and the point in phase space at

which the density is being evaluated. The parameter α is determined by demanding that phase space is as close to the saturation value as possible for a cold nucleus (this gives $\alpha = 0.5$ fm^{-1}). The nuclear potential at any given position can be evaluated by determining the nuclear density at that position by summing over the Gaussian density distributions of all nucleons.

In the model, individual nucleons are also allowed to scatter from each other in a manner similar to the Boltzmann collision term. The scattering is handled stochastically: at the distance of closest approach, a pair of nucleons scatter into new momenta chosen randomly from a predetermined distribution in angle. At these energies, the scattering is isotropic in the centre-of-mass frame. The magnitude of the NN cross section is taken from the experimental data in the 100-300 MeV bombarding energy range where the cross section is observed to be approximately constant. The rise in the cross section at low momentum (where the cross section goes like p^{-2}) is assumed to be included in the attractive part of the nuclear mean field. The scattering process provides a mechanism for the incorporation of the Pauli exclusion principle in the Uehling-Uhlenbeck sense: once the new momenta for the members of the scattering pair are chosen, the fractional occupancy of the new points in phase space (f_1 and f_2) is checked. A random number is chosen and compared to

$$u = (1 - f_1) \times (1 - f_2) \tag{3}$$

The collision is allowed or forbidden according to the value of the random number chosen. To the extent that the collisions are fast, this technique can be used to mimic the Pauli exclusion principle and keep nucleons from moving too far into regions of phase space which are forbidden.

The calculational technique of the model bears close resemblance to that of the Boltzmann-like equations used to solve for the time evolution of one-body distributions of fermions. Hence, an average over the individual events generated by the model should yield similar results to those found from the corresponding kinetic equation. Because of the fluctuations in phase space present in the model at low excitation energies (since the wavefunctions are not that accurately represented by single Gaussians) the model will be of limited use in describing some aspects of low energy reactions or processes which involve excitation energies of a few MeV per nucleon. Similarly, because the collision term is the only way Fermi-Dirac statistics are incorporated in the model, the existence of small local fluctuations in phase space implies that there is a small, but finite, probability that a pair of nucleons can scatter even though they will be propagated into regions of phase space which, on average, are

saturated. Thus, over long times there will be "artificial" evaporation of nucleons and the model is not appropriate for the evaluation of evaporation-like processes. Of course, kinetic equations are not generally applied to the study of evaporation processes because each event would have to be followed for a prohibitively large number of time steps.

Bearing these caveats in mind, we now attempt to develop an intuitive picture for the reaction mechanisms of proton and heavy ion induced reactions at intermediate energy. All collisions to be discussed are at zero impact parameter. The first reaction of interest is p + Ag at 300 MeV. The coordinate space positions of the nucleons in a single collision are shown in Figure 1. The event is shown at three time steps: 1, 100 and 150 fm/c. In this particular event, the incoming proton has been stopped in the target and its energy has become distributed among the target nucleons (this is not always the case in central collisions of proton induced reactions and is even less likely in peripheral ones). Although it cannot be seen from the figure, the target is observed to oscillate in time, and finally begin to break apart on the time scale of hundreds of fm/c.

The central collision of two calcium nuclei at a bombarding energy of 25 MeV/nucleon is a more energetic process, as is evidenced by Figure 2. One can see that the nuclei largely fuse, although the fused system has a high excitation energy and breaks up on a shorter time scale than does the p+Ag system. However, if one raises the bombarding energy further to 50 MeV/nucleon, breakup is both rapid and extensive. This is illustrated in Figure 3. As the energy is raised beyond 50 MeV/nucleon, destruction of the nuclei becomes more complete in central collisions, particularly at bombarding energies beyond 100 MeV/nucleon. We will use these three reactions, then, as representational of the change from binary-fission-like decay to multifragmentation. In the centre of mass frame, the total kinetic energy per nucleon is about 3, 6 and 12 MeV for Figures 1-3 respectively.

As far as multifragmentation is concerned, what the simulations show is that the fluctuations which develop early in the reaction are propagated through the expansion regime and emerge as fragments as the reaction zone goes out of equilibrium. The simulations do not show the formation of a hot gas from which fragments coalesce late in the reaction. This point will be made more quantitative in Section 4. It is also clear that the nuclear surface tension plays a strong role in fragmentation.

Since the simulations purport to contain meaningful phase space fluctuations, in principle they can be used to calculate any experimental variable desired, subject to the availability of computer time. Only one illustrative example will be shown here, namely the isotopic yields of light fragments.

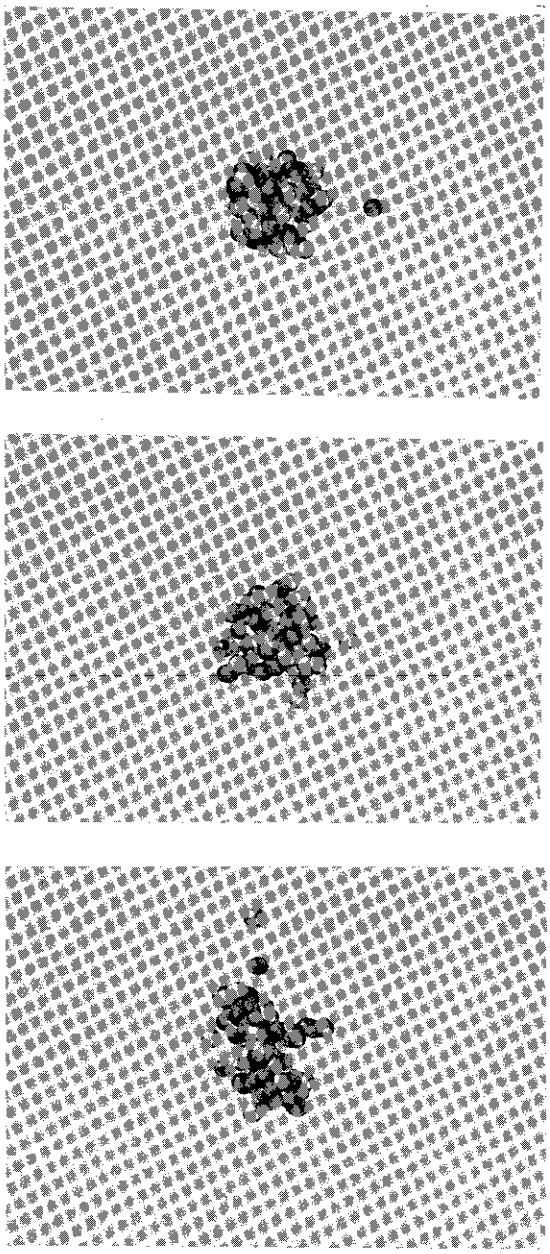

FIGURE 1
Time evolution of a central p + Ag collision at 300 MeV bombarding energy. The reaction is shown at 1,100 and 150 fm/c elapsed time. The dark spheres represent protons while the light ones are neutrons.

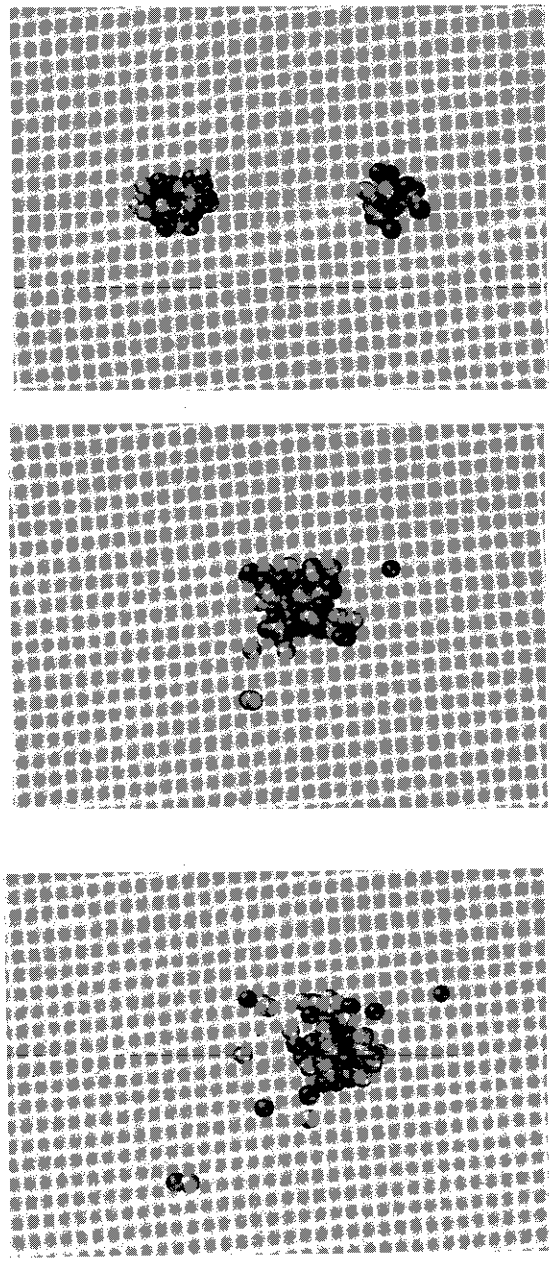

FIGURE 2
Time evolution of a central Ca + Ca collision at 25 MeV/nucleon bombarding energy. Same representation as Figure 1.

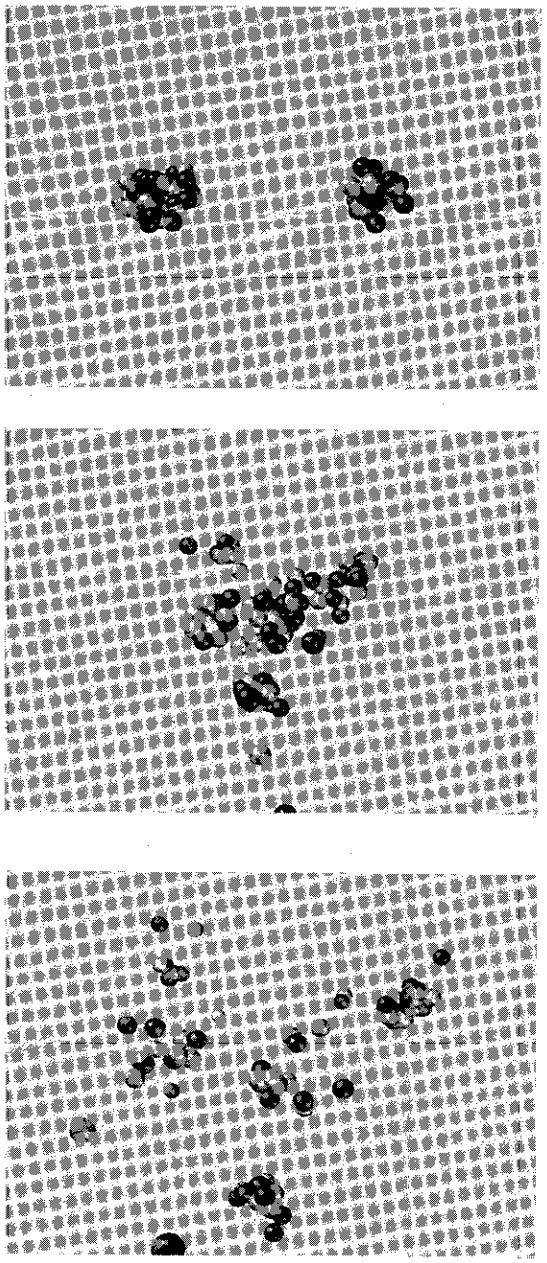

FIGURE 3
Time evolution of a central Ca + Ca collision at 50 MeV/nucleon bombarding energy. Same representation as Figure 1.

These are shown in Figure 4 for each of our chosen reactions. All of the distributions show a rapid falloff as one moves away from the N=Z line. This is a result both of the isospin dependent interaction in the mean field and of the combinatorics of choosing a given fragment Z and N from the parent system. In any event, were one to do a fit to these yields with a chemical equilibrium model containing a "chemical" temperature as a parameter, a low temperature would be obtained. Comparing one reaction type with another, one can see that the yields fall much more rapidly with increasing mass in the proton induced reaction than they do in the other reactions. Further, from both the width of the distribution around N=Z and the falloff with mass, one can see that the chemical temperature is increasing with excitation energy of the system, as one would expect. Lastly, it should be mentioned that the yields typically agree with the data at the factor of two level (detailed comparison of the predicted yields with data is difficult since the model cannot be expected to produce fragments with the correct binding energy, particularly for light fragments).

3. LIQUID-GAS PHASE TRANSITION

The nucleon-nucleon interaction is repulsive at short distances and attractive at large distances, a behaviour which is qualitatively similar to the molecular interaction of substances which exist in liquid and gaseous phases. This similarity suggests that infinite neutral nuclear matter may also exist in distinct liquid and gas states with a phase boundary between them[11-15]. To extract the essential features of the equation of state, we will adopt a simple model[16-18] in which the nucleon-nucleon potential is approximated by a zero-range Skyrme-type interaction:

$$V_{12} = \left[-t_o + \frac{t_3}{6}\,\rho\delta(\vec{r}_1-\vec{r}_2)\right] \tag{4}$$

where ρ denotes the density at $(\vec{r}_1+\vec{r}_2)/2$ for nucleons at positions $\vec{r}_1$ and $\vec{r}_2$. The parameters t_o and t_3 which appear in Equation 4 are chosen to fit the properties of cold nuclear matter. The potential energy associated with this interaction has the form

$$U(\rho) = -\frac{3}{4}\,t_o\,\rho + \frac{3}{16}\,t_3\,\rho^2 \tag{5}$$

which are just the first two terms in Equation 1. The pressure can be calculated for this interaction and, by Maxwell's construction, the phase diagram.

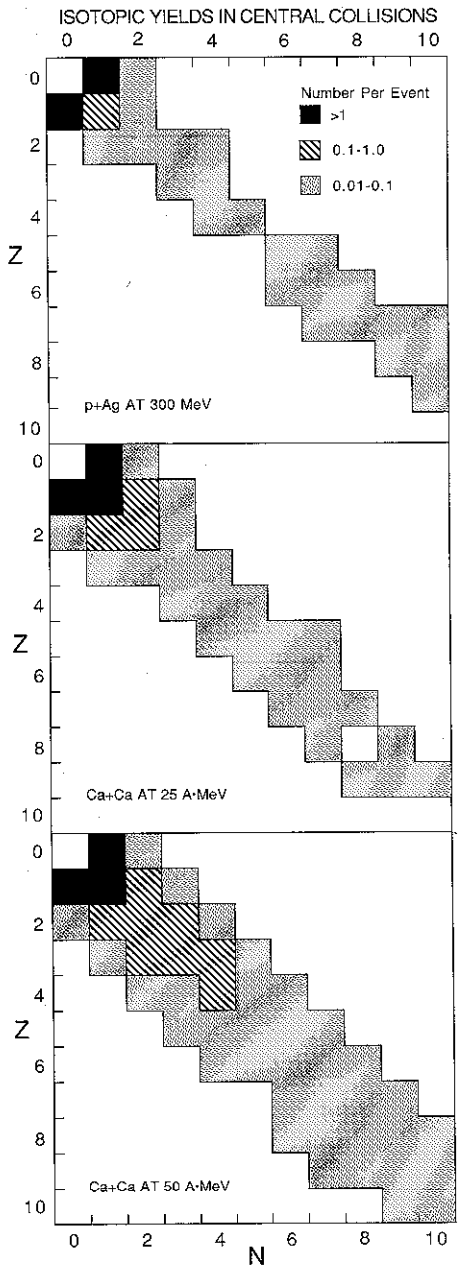

FIGURE 4
Isotopic yields in the light to medium mass fragment range for the reactions shown in Figures 1-3. The yields are given as the number of fragments of a given Z,N per event (From 7).

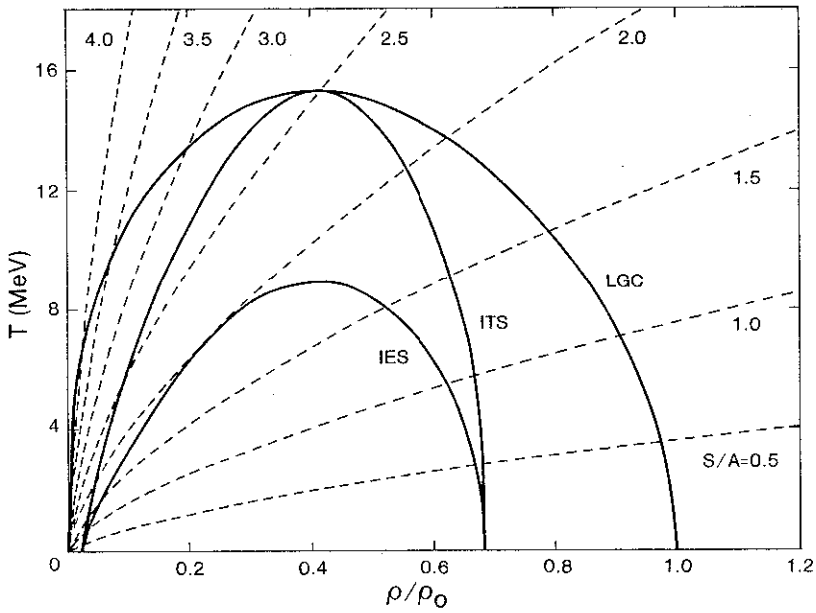

FIGURE 5
Phase diagram of neutral nuclear matter associated with a zero range Skyrme-type interaction. Isentropes of given values of the entropy per nucleon (S/A) are shown by the dashed curves. The liquid-gas coexistence curve is labelled as LGC; the isothermal and isentropic spinodals are labelled as ITS and IES respectively (From 16).

The resulting phase boundaries are shown in Figure 5: the liquid-gas coexistence curve is labelled by LGC while the isothermal and isentropic spinodal curves (defined by $(\partial P/\partial \rho)_T = 0$ and $(\partial P/\partial \rho)_S = 0$ respectively) are labelled by ITS and IES. Also shown in the figure are curves of constant entropy.

The boundaries of the phase diagram are not particularly sensitive to the specific choice of parametrization of the nucleon-nucleon interaction; rather similar results were obtained by 16 and 18 using different parametrizations. However, the inclusion of the coulomb interaction and other effects lowers the predicted value of the critical temperature considerably[19].

How well do the phase properties of infinite nuclear matter shown in Figure 5 carry over to real nuclei, which are small and evolve with time if they are not in their ground state? The question of the effects of phase boundaries on rapidly evolving inhomogeneous systems such as are produced in a reaction will be dealt with in the next section. Here, we wish to address the more restricted question of the evolution of single nuclei with a specific initial compression and temperature.

The approach taken to investigate this problem will again involve the use of computer simulations. The specific aspect of the problem on which we will focus is fairly narrow: as a "real" nucleus at a specific initial temperature and rms radius evolves with time, does the existence of the mechanical instability region effect how it deexcites? The experimental observable which will be used to measure the nature of the breakup mode will be the mass distribution as observed at a fixed time (150 fm/c) after the initial configuration is released. The computational model[20] used for the investigation is in many aspects more primitive than the one outlined in the previous section; the major simplification is the omission of the collision term. This implies that the 1-body distributions predicted by the model will evolve approximately like the Vlasov equation, which is not a bad approximation for single nuclei at low excitation but is inappropriate for collisions. The full model including collisions is used everywhere else in this paper.

In the simulations, a mass 100 system was chosen as the test nucleus. In each initialization, the nucleons were distributed in momenta according to a finite temperature Fermi distribution. In coordinate space, the nucleons were distributed according to a Woods-Saxon distribution of fixed width parameter. The initial compression was varied by changing the half-density radius R. For the density-dependent potential used in the calculation[20], which was slightly different from Equation 1, the zero temperature ground state of this system was found to be at R=5.2 fm. The mass yields were determined by following a sample of 100 nuclei initialized (in a Monte Carlo sense) at a set T-R combination.

Raising the temperature with R fixed at 5.2 fm., the mass distribution shows increasing particle emission. Particle loss becomes greater as the temperature passes the critical point, but no large discontinuity in the shape of the yield curve is observed. This is, of course, to be expected for small systems, where fluctuations may blur the critical point dramatically. However, if the temperature is kept constant at 0 MeV, but the system is compressed by decreasing R, a very different behaviour emerges. This is shown in Figure 6.

At small compressions, the system basically oscillates around the equilibrium density, slowly losing particles. As one can see from the figure, there is a very dramatic change as the initial compression increases past about 30% above normal nuclear matter density. Here, the system no longer oscillates, but simply expands and breaks apart. In infinite matter, this would correspond to reaching the overstressed zone, whose boundary was pointed out by Bertsch and Siemens[21]. Systems which start off from within this zone have sufficient energy to pass into the mechanical instability region ($\partial P/\partial \rho < 0$) as they expand, leading to breakup of the system. In the finite systems considered

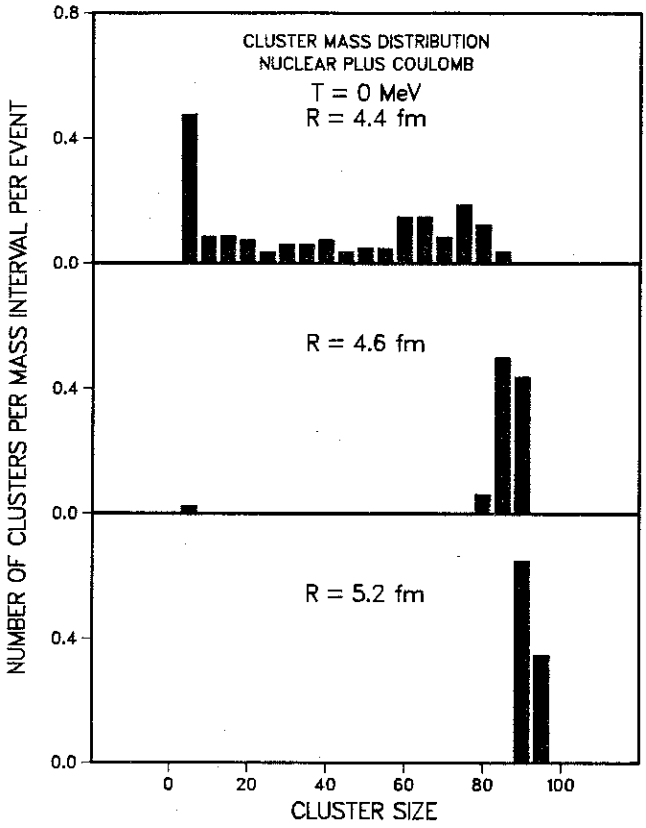

FIGURE 6
Mass distributions predicted in a collisionless semiclassical simulation for a mass 100 system initially at zero temperature and various densities. See text for discussion of method (from 20).

here, this boundary remains relatively sharp. One would also expect it to be at slightly lower density than what is observed for infinite matter, since the finite spatial size of the system means that fast particles can rapidly escape from it, depleting the density and leaving voids in the nucleus.

It should be checked to ensure that the reaction products are actually exhibiting liquid-like behaviour associated with the long range attraction and short range repulsion of the nuclear mean field. While we have not analyzed this problem completely, one step on the way is to examine the two particle correlation function in coordinate space $C(\vec{r}_1,\vec{r}_2)$. We define this via:

(6) $$C(\vec{r}_1,\vec{r}_2) = N_0 N(\vec{r}_1,\vec{r}_2)/N(\vec{r}_1)N(\vec{r}_2)$$

where $N(\vec{r}_1,\vec{r}_2)$ is the number of coincident pairs of nucleons at positions $\vec{r}_1$ and $\vec{r}_2$ while $N(\vec{r})$ is the total number of nucleons at position $\vec{r}$. There is an overall normalization factor N_o to ensure that $C(\vec{r}_1,\vec{r}_2)$ goes to unity as Δr goes to infinity. In numerical simulations, the nucleon positions are, of course, segregated into finite bins in coordinate space for the purpose of the analysis. It is more convenient to replace the denominator in Equation 6 by a number of pairs generated by randomly choosing nucleons from different events. This event mixing technique allows one to avoid many of the difficulties imposed by having to match up bin sizes in the numerator and denominator.

What one would expect to see is a depletion in the correlation function at small relative separation arising from the short range repulsion, and then a strong enhancement at separations typical of the average separation in the liquid drops. At larger separations, there again should be a suppression of the correlation function, since nucleons slightly outside the drop's surface should be pulled inside by the force (in addition, they will be repelled by the charge, if they are charged or are residing in other charged drops). The results for two of the reactions considered in the previous section are shown in Figure 7.

The suppression at very short distances is not observable in the figure because of the limited statistics of the data sample. However, the enhancement at separations of a few fm, and the suppression at scales of tens of fm is obvious. Further, since the actual droplets in the proton induced reaction are fairly large, this gives a good standard against which the smaller droplets formed in the heavy ion reaction can be compared. The fact that the two correlation functions are so similar is in agreement with our picture that the droplets are not just random coincidences of particles in a non-interacting gas.

Hence, the simulations show that some of the features of the infinite matter phase boundaries do survive in dynamically evolving finite systems, although there are modifications which may be significant. However, even the finite system investigated in this section is idealized compared to the reaction region produced in a collision, and the search for phase transition effects in such a region is bound to be more difficult.

4. REACTION TRAJECTORIES

In the previous sections, the final reaction products of the computer simulations have been used to demonstrate two points: that the simulations agree at least at the semi-quantitative level with experimental measurements, and that even in finite dynamically evolving systems, features of the infinite matter

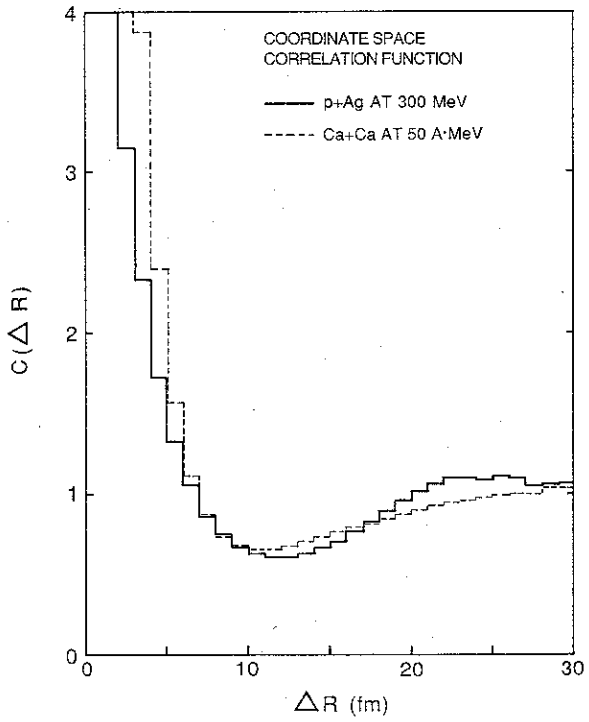

FIGURE 7
Coordinate space correlation function calculated for the reaction products at an elapsed time of 150 fm/c. Two reactions at zero impact parameter are shown: p + Ag at 300 MeV and Ca + Ca at 50 MeV/nucleon (From 7).

phase boundaries survive. However, the real power of the simulations is that they allow the time evolution of the reaction volume to be investigated in detail. We will now use the simulations to look inside the reaction region, so to speak, and see how the physics of the phase transition manifests itself.

The method is the following: During each event of the simulation, the positions and momenta of each nucleon are stored every 10 fm. At the end of the event, a cluster search is performed and it is determined to which cluster, if any, each nucleon belongs (where the clusters are defined by the minimum separation criterion. See 6). By tracing back through the stored positions and momenta, the local coordinate and phase space density through which each nucleon passed on its way through the reaction can be determined. Averaging over many events, one can determine the average local densities traversed by nucleons which ultimately emerge in a given cluster mass. The time evolution of the average coordinate space density is shown in Figure 8 for the reactions of

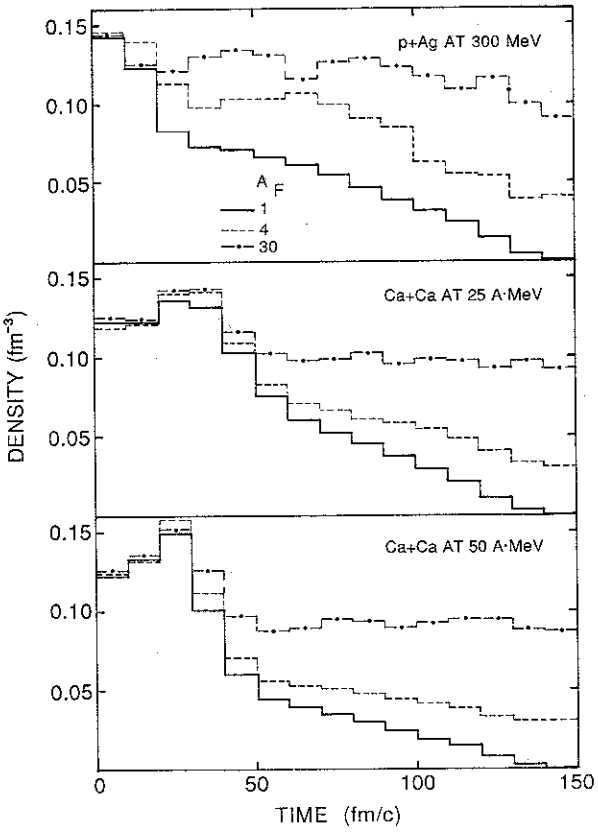

FIGURE 8

Time evolution of the average local coordinate space density in the vicinity of nucleons which finally emerge from the reaction as free nucleons (A=1) or in bound clusters (A=4,30). Results are shown for the reactions in Figures 1-3 (From 7).

Figures 1-3. Three sample cluster masses are shown: A=1,4 and 30.

First, some general comments on the figure. In the proton induced reaction, one observes that the fall-off of the density with time is slower than what is observed for the heavy ion reactions. Intuitively, we would expect that with such a low excitation energy, the processes in this reaction would be very slow compared to the heavy ion reactions , as was pointed out earlier in the discussion of Figures 1-3. Further, it would appear that the density falls off more slowly as the charge of the emitted fragment increases, which would be expected because of the coulomb barrier. This interpretation can be strengthened by determining an "emission time" for each fragment and comparing emission rates

between fragment masses. This is shown in Figure 9.

The emission time in these simulations is defined as the first time step (binned in 10 fm/c steps) at which the average local density observed by nucleons which ultimately emerge as the fragment falls below 0.08 fm^{-3}. While this choice is a little arbitrary, it will do. What is shown in the figure is then the average emission rate for A=1 and 4 as a function of time. Fragments with lower charge tend to be emitted earlier in the reaction than those with larger charges, and, since nucleons are more copiously produced than fragments, their emission rate is higher.

Having confirmed the interpretation of the time evolution of the quantities in Figure 8, we return to comment on their significance to the phase transition question. From both Figure 8 and the coordinate space evolution shown in

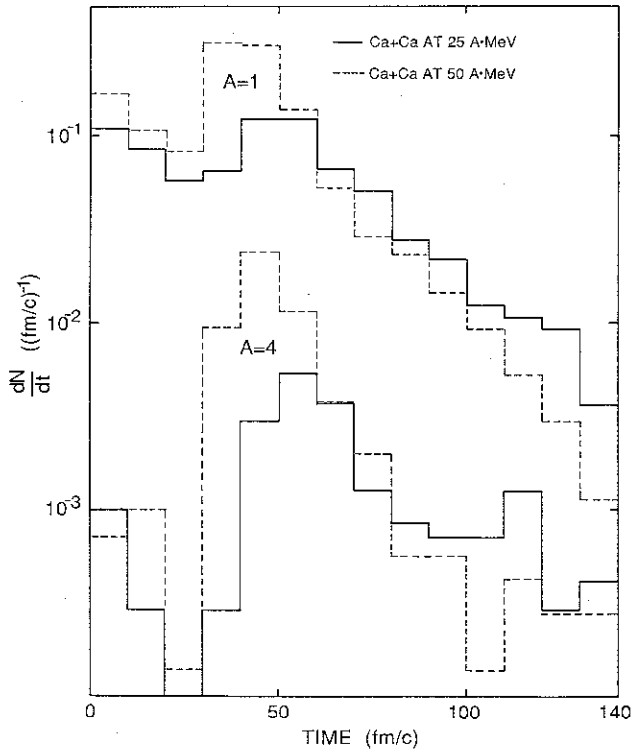

FIGURE 9
"Emission rate" of nucleons and A=4 clusters in the reactions shown in Figures 2 and 3. In the simulation, the emission time is defined as the time when the average local coordinate space density observed by nucleons in a cluster first drops below 0.08 fm^{-3} (From 7).

Figures 1-3, density fluctuations play an important role in determining which nucleons will emerge in clusters. Nucleons which are scattered into low coordinate density regions tend to emerge as free particles. This observation is strengthened if one plots phase space density instead of coordinate space density (see 6,7): nucleons which emerge as free particles in energetic reactions are scattered into low density regions of phase space early on in the reaction, before they begin to separate in coordinate space. Hence, the fluctuations produced early in the reaction tend to be propagated through it. Further, from the behaviour of the mass 30 densities in Figure 8, one observes that the average local density does not drop below some minimum value. In fact, this behaviour is observed in the simulations for a wide range of fragment masses and is what is expected from the existence of the mechanical instability region: if the local density falls below a minimum value, the system breaks apart, otherwise it recontracts and oscillates. In the reactions studied here, the minimumdensity appears to be about half nuclear matter density at low excitation energy.

From studying these three illustrative reactions, we observed the following about the reaction trajectories: At low excitation energies, the system oscillates around the coexistence region, slowly losing particles. As the excitation energy is raised, the system may enter the mechanical instability region and fragment into pieces, depending on the the energy involved. At higher energies, the system may vaporize, but even in the vaporization process at the energies studied, the system does not fall to very low densities from which fragments condense; the higher density regions survive throughout the reaction.

These observations from the time evolution manifest themselves in experimental observables such as the correlation in fragment masses. We show in Table 1 the probability of obtaining a pair of fragments of mass A_1 and A_2 in a central collision. The mass bins are taken to be fairly large: 8 mass units. As one would expect, the probability of obtaining a pair of light fragments is unity in all three reactions. The probability decreases as the fragment mass increases, in general. However, in the lower energy reactions, one can see an enhancement along the binary fission line. The effect is more pronounced in the mass correlation function, defined by:

$$C(A_1,A_2) = N_0 N(A_1,A_2)/N(A_1)N(A_2) \tag{7}$$

where $N(A_1,A_2)$ is the number of coincident pairs of fragments of mass A_1 and A_2 which are produced, $N(A)$ is the number of fragments of mass A produced in the

Table 1. Predicted probability for finding a pair of fragments in an event as a function of fragment masses. Each mass is binned in eight mass units (from 7).

p + Ag at 300 MeV

	8	16	24	32	40	48	56	64	72	80
8	0.992	0.154	0.177	0.125	0.095	0.080	0.069	0.072	0.072	0.092
16	0.154	0.021	0.025	0.020	0.012	0.009	0.011	0.009	0.016	0.012
24	0.177	0.025	0.014	0.026	0.012	0.011	0.025	0.010	0.011	0.040
32	0.125	0.020	0.026	0.004	0.014	0.019	0.019	0.014	0.022	0.045
40	0.095	0.012	0.012	0.014	0.007	0.012	0.016	0.021	0.035	0.001
48	0.080	0.009	0.011	0.019	0.012	0.002	0.020	0.030	0.002	
56	0.069	0.011	0.025	0.019	0.016	0.020	0.005	0.004		
64	0.072	0.009	0.010	0.014	0.021	0.030	0.004			
72	0.072	0.016	0.011	0.022	0.035	0.002				
80	0.092	0.012	0.040	0.045	0.001					

Ca + Ca at 25 MeV/nucleon

	8	16	24	32	40	48	56	64	72	80
8	0.997	0.329	0.180	0.159	0.129	0.125	0.142	0.195	0.230	0.097
16	0.329	0.067	0.071	0.066	0.063	0.044	0.076	0.071	0.014	0.001
24	0.180	0.071	0.017	0.036	0.047	0.047	0.035	0.004		
32	0.159	0.066	0.036	0.029	0.045	0.037	0.002			
40	0.129	0.063	0.047	0.045	0.009	0.004				
48	0.125	0.044	0.047	0.037	0.004					
56	0.142	0.076	0.035	0.002						
64	0.195	0.071	0.004							
72	0.230	0.014								
80	0.097	0.001								

Ca + Ca at 50 MeV/nucleon

	8	16	24	32	40	48	56	64	72
8	1.000	0.615	0.366	0.272	0.225	0.160	0.100	0.060	0.014
16	0.615	0.236	0.225	0.165	0.149	0.089	0.040	0.005	
24	0.366	0.225	0.087	0.111	0.061	0.021	0.001		
32	0.272	0.165	0.111	0.027	0.025	0.002			
40	0.225	0.149	0.061	0.025	0.001				
48	0.160	0.089	0.021	0.002					
56	0.100	0.040	0.001						
64	0.060	0.005							
72	0.014								

sample and N_o is a normalization constant. As before, we construct the correlation function by the event mixing method. The predictions for the three reactions are shown in Figure 10. There is a very large enhancement along the binary fission line for the p+Ag reaction, the correlation function rising to about 4 for the mass bins chosen. For the 25 MeV/nucleon Ca+Ca reaction, the enhancement has been substantially reduced, at least partly reflecting the fact that one is not beginning the reaction with a large system but rather must form

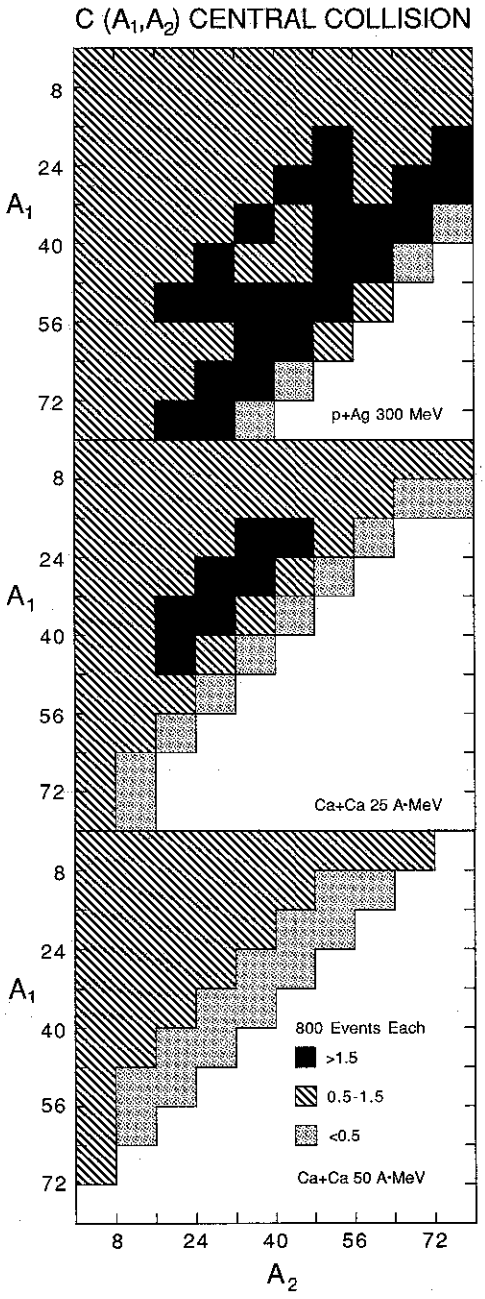

FIGURE 10
Mass-mass correlation function predicted for the reactions shown in Figures 1-3. The fragment masses are grouped in bins of eight mass units (From 7).

it during the reaction. By 50 MeV/nucleon, the enhancements have largely disappeared. Raising the bombarding energy beyond 50 MeV/nucleon continues to lower the yield of heavy fragments, but does not result in any new structure in the correlation function with the mass resolution used.

5. SUMMARY

A semiclassical model for use in the computer simulation of nuclear reactions at intermediate energy is been presented. With it, an intuitive picture of the excitation energy dependence of fragmentation processes is developed. At low energies, fragmentation is shown in the simulations to be a long time scale process involving a binary fission. At higher excitation energies, the system breaks up into larger numbers of fragments, and finally vaporizes at the highest energies. The simulations are also used to demonstrate that the phase transition-like behaviour associated with infinite matter is also present in dynamically evolving single nuclei of varying initial temperature and compression.

By using the simulations to investigate the reaction trajectories of nucleons in coordinate and phase space as they emerged as fragments from the reaction zone, it was shown that phase transition-like effects were present even in the inhomogeneous systems produced in reactions. Evidence was presented for the existence of a minimum density defining the boundary of a mechanical instability region: if the local density of a region dropped below this threshold density, the material broke up; otherwise it could recontract. While experimental determination of the boundaries of the instability region remains elusive, nevertheless it was shown that the two-particle correlation function in fragment mass should possess a clearly visible energy dependence reflecting the physics of the instability.

ACKNOWLEDGEMENTS

The authors wish to thank the Graphics Laboratory of Simon Fraser University for much patience and guidance in the preparation of the computer animations presented at this meeting. This work was supported in part from a grant from the Natural Sciences and Engineering Research Council of Canada.

REFERENCES

1) D.H. Boal, Computer simulations of nuclear dynamics, in: Annu. Rev. Nucl. Part. Sci., Vol. 37, eds. J.D. Jackson, H.E. Gove and R.F Schwitters (Annual Reviews, Palo Alto, 1987).

2) J. Cugnon, Lectures given at the Cargese Summer School (1984).